Biochemical and Biophysical Research Communications 377 (2008) 79–84

Contents lists available at ScienceDirect

Biochemical and Biophysical Research Communications

journal homepage: www.elsevier.com/locate/ybbrc

A high contrast method of unstained biological samples under a thin carbon film by scanning electron microscopy

Toshihiko Ogura *

Neuroscience Research Institute, National Institute of Advanced Industrial Science and Technology (AIST), Central 2, Umezono, Tsukuba, Ibaraki 305-8568, Japan
PRESTO, Japan Science and Technology Agency, 4-1-8 Honcho Kawaguchi, Saitama, Japan

ARTICLE INFO

Article history:
Received 16 September 2008
Available online 1 October 2008

Keywords:
Scanning electron microscopy
Biological sample
Bacteria
Secondary electron
Low acceleration voltage
Carbon film
Lower surface

ABSTRACT

The contrast of biological samples in scanning electron microscopy (SEM) is very weak. To examine a biological specimen by SEM, many steps and/or special equipment are required to prepare the sample. Here, we describe a method using an unstained biological sample under a 40 nm carbon film to give a high contrast image, where the image is detected by the secondary electron (SE) signal at a low accelerating voltage of 1.5 kV. Under these conditions, it is hard to detect a direct signal from a biological specimen. The high contrast image is created by the SEs from the lower surface of the thin carbon film. Therefore, the damage to the sample from the electron beam is very low. Our method can be utilized to observe various biological samples of bacteria, viruses, and protein complexes.

Scanning electron microscopy (SEM) is a useful technique for the investigation of surface structure of biological samples [1–3]. To allow observations under the high vacuum conditions of SEM, many preparations of biological samples have been developed, e.g., glutaraldehyde fixation, negative staining, the Sputter–Cryo technique, and coating with gold or osmium [4–7]. Moreover, these preparations have some positive effects on the biological sample; for instance, they enhance contrast, reduce damage, and are uncharged up by the electron beam. Using these techniques, various bacteria have been observed [4,7,8]. However, these preparations require many steps and/or special equipments. Therefore, a more convenient preparation method for biological samples is needed.

Here, we show that an unstained biological sample under a thin carbon film gives a high contrast detected by the secondary electron (SE) signal at a low accelerating voltage of 1.5 kV. The bacteria sample is attached to the lower surface of a 40 nm carbon film. However, the electron beam radiates to the top of the carbon film, making it hard to detect a direct signal from the sample. Therefore, the high contrast images obtained here are generated by an indirect mechanism. In this paper, we investigate the high contrast mechanism under various conditions. Further, we propose a new high contrast technique based on our experimental results.

Material and methods

Sample preparation. Bacterial samples were obtained from the dental plaque of a male in his late thirties. A piece of plaque was taken by the wood tooth pick which was sterile by 70% ethanol. The plaque was dissolved in 50 μl distilled water in a 2 ml tube using a pipetman (Gilson, France). To ascertain the presence of bacteria, a sample of the solution was observed using an optical microscope (Eclipse E100, Nikon, Japan) before preparation for the SEM. To prepare the SEM sample, 3 μl of the sample solution was dropped onto a thin elastic-carbon film, with a thickness of approximately 40 nm, supported by a copper mesh grid (STEM150 Cu grid, OkenShoji Co., Japan). After 3 min, the samples were washed with distilled water, and dried at room temperature (23 °C).

Scanning electron microscopy. The mesh grid supporting the bacteria was attached at the center of a 2.5 mm diameter hole on an aluminum sample holder using carbon tape, with a hole in the same position as that of the holder (Fig. 1A). The sample holder with the grid was fixed onto an aluminum stage (Fig. 1B). From the lower side of the carbon film, the sample holder was reversed vertically. The sample stage was transferred to the chamber of a

Abbreviations: SEM, scanning electron microscopy; SE, secondary electron; 3D, three-dimensional.

* Address: Neuroscience Research Institute, National Institute of Advanced Industrial Science and Technology (AIST), Central 2, Umezono, Tsukuba, Ibaraki 305-8568, Japan. Fax: +81 29 861 5065.
E-mail address: t-ogura@aist.go.jp

0006-291X/$ - see front matter © 2008 Elsevier Inc. All rights reserved.
doi:10.1016/j.bbrc.2008.09.097

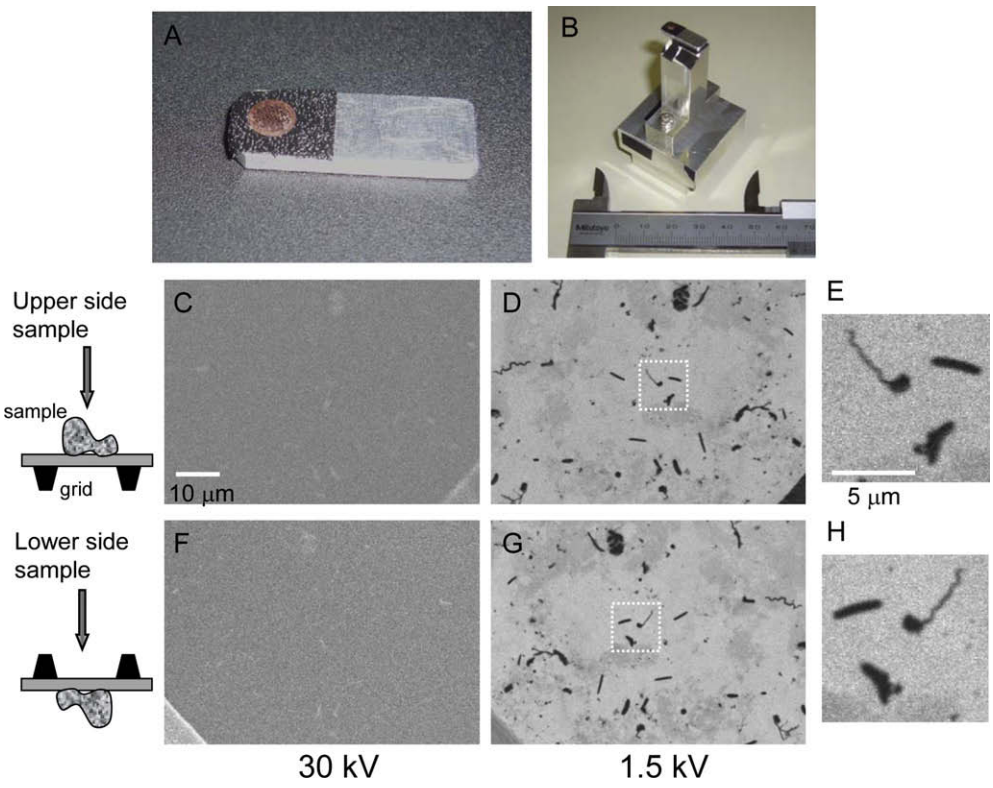

Fig. 1. Comparison of SEM images of the bacterial sample from the upper and lower side of the 40 nm elastic-carbon film. (A) Photograph of an aluminum sample holder with an elastic-carbon film supported by a copper grid mesh. A grid with the bacteria is attached to the center of 2.5 mm diameter hole of a sample holder. (B) A sample holder with a grid is fixed onto an aluminum stage. (C) SEM image of the bacterial specimen on the carbon film taken at 30 kV. The bacteria are shown in very weak white contrast. The scale bar represents 10 μm. (D) SEM image of the upper side of the sample taken at 1.5 kV. The various bacteria are shown in clear black contrast. *F. nucleatum*, *T. denticola*, *S. flueggei*, and *P. gingivalis* [8–14] are clearly identifiable in the high contrast image. (E) Expanded image of the area enclosed by the white dashed square in (D). The scale bar represents 5 μm. (F) Image of the bacteria under the thin carbon film at 30 kV, showing the same area as (C). The bacteria are shown in very weak white contrast, as in (C). (G) Image taken by the bacteria under the thin carbon film at 1.5 kV. The bacteria are shown in very clear black contrast as in (D). (H) Expanded image of the area enclosed by the white dashed square in (G).

thermionic emission type SEM (JSM-6390, JEOL, Japan). All images were taken with an SE signal under high vacuum conditions.

Results

The bacterial specimen on the elastic-carbon grid was attached to an aluminum holder (Fig. 1A), which was also fixed to a stage (Fig. 1B). The sample images were observed with the SEM using the SE signal. The bacteria on the carbon film were first observed at 30 kV (Fig. 1C). Under this condition, the bacteria appeared in faint white contrast. Thus, it was hard to identify the structure of bacteria (Fig. 1C). Under a low acceleration voltage of 1.5 kV, the bacteria had a very clear black contrast. Therefore, it was easy to identify the various bacteria on the carbon film (Fig. 1D and E). The oral bacteria viewed, which were identified according to their form, were as follows: *Fusobacterium nucleatum*, *Treponema denticola*, *Selenomonas flueggei*, and *Porphyromonas gingivalis* [8–14].

For the next condition investigated, the sample was placed under the carbon film, which is not a conventional setting for SEM. A high acceleration voltage of 30 kV was used, as shown in Fig. 1F. The image obtained is similar to the upper side sample in Fig. 1C. At this acceleration voltage, many electrons hit the lower side of the sample by scattering through the thin carbon film. Therefore, the lower side sample image is similar to the white contrast of the upper side image. On the other hand, at a low acceleration voltage of 1.5 kV, many electrons are absorbed by the thin carbon film [15,16]. A clear and high contrast image of bacteria was observed under this condition (Fig. 1G and H). Interestingly, this image is very similar to the upper side sample (Fig. 1D and E). Under this condition, it is hard to detect the direct signal from the lower side sample.

To investigate the high contrast mechanism for the lower side sample, the acceleration voltage was varied between 30 and 0.7 kV (Fig. 2). The bacterial images between 10 kV from 30 kV showed white contrast (Fig. 2A–C). At 10 kV, the white contrast reached a maximum. However, the detailed form of the bacteria was difficult to observe in this image. At 5.0 kV, the bacterial image disappeared because of lack of contrast (Fig. 2D). At a lower acceleration of 5.0 kV, the bacteria gradually emerged in black contrast again (Fig. 2E and F). At 1.5 kV, the image had a clear black contrast, which enabled the bacteria to be observed in detail (Fig. 2G). As the acceleration lowered to 1.5 kV, the clear contrast gradually disappeared (Fig. 2H and I). These results showed two contrast peaks; white at 10 kV and clear black at 1.5 kV.

To examine the damage to the sample under the carbon film caused by an electron beam at 1.5 kV, the same sample was scanned many times. The first scanned image is shown in Fig. 3A; the bacterium has three flagella and a dome-like body. Images of the same bacterium were taken four times at a magnification of 10,000×. Further five images were taken at 20,000× magnification. The final image after a total of nine scans is shown in Fig. 3B; it is similar to the first image (Fig. 3A and B). Therefore, there is little damage to the sample under the carbon film from the electron beam. Next, to investigate the first scanned image in detail, we made a pseudo-color image and a three-dimensional (3D) map of the first scanned image, Fig. 3C and D. The body of the bacterium is dome-shaped. Moreover, the brightness of the crossover points of the flagella is two times higher than the other flagella positions (Fig. 3C and D white arrow). These results suggest that the lower sample image was similar to a transmission image, depending more on the sample volume than its surface, as in general SEM. If the image

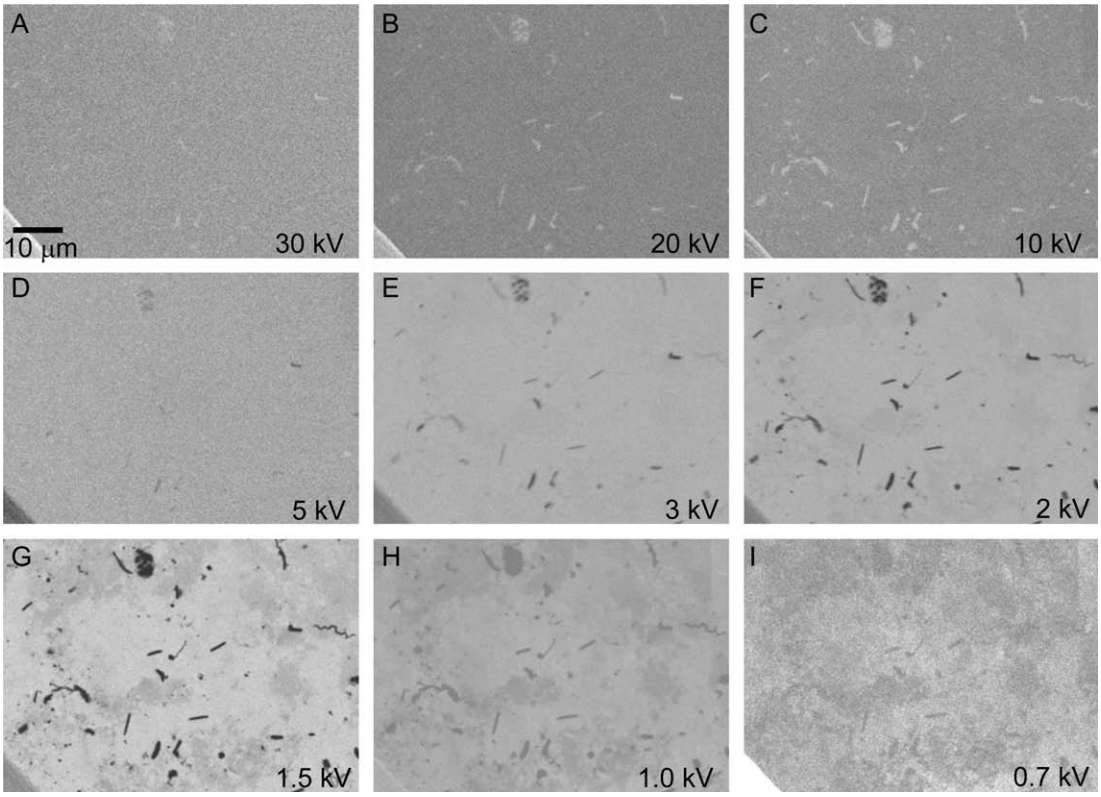

Fig. 2. Comparison of the images of the bacterial specimen under a carbon film obtained from various accelerations. (A) Image obtained from an acceleration voltage of 30 kV, which shows very weak white contrast. The scale bar represents 10 μm. (B) Image of the bacteria under the thin carbon film at 20 kV, the white contrast is higher than that at 30 kV. (C) Image obtained at 10 kV; at this voltage, the white contrast of bacteria peaks. (D) Image obtained at 5 kV, the sample contrast disappears. (E) Image of large rod-type bacteria showing weak black contrast at 3 kV. (F) Image at 2 kV; the black contrast starts to increase. (G) Image obtained at 1.5 kV; the black contrast of bacteria is at its maximum, allowing easy identification of the various bacterial structures. (H) Image obtained at 1.0 kV, the black contrast begins to decrease. (I) Image obtained at 0.7 kV, the black contrast has almost disappeared.

obtained by our method is equivalent to the transmission image, it would enable the reconstruction of a 3D model using a tilting stage. A comparison of images from the flat stage and the 30° tilt of the sample is shown in Fig. 3E and F. The aspect of the bacterium is changed by the tilt stage. In particular, its body and flagella are characteristically shifted. Therefore, our method allows reconstruction of 3D models using many tilted images.

Finally, we examined the high contrast mechanism from the lower side of the film (Fig. 4). With an open bottom space, both sides of the sample showed very clear contrast at 1.5 kV (Fig. 4A and B), as in Fig. 1–3. On the other hand, with a bottom space closed by an aluminum tube, the bacterial image disappeared (Fig. 4C and D). These results strongly suggest that the high contrast mechanism is generated from the lower surface of the carbon film (Fig. 4E).

Discussion

The interaction of the electron beam with light materials is weaker than that with heavy materials [17]. Therefore, the contrast of biological sample images from SEM is very weak. To observe biological specimens with a SEM, the preparation of the sample requires many steps and/or special equipments [1,4–6]. Therefore, a more convenient method of preparing the sample would be very useful. In the present study, a high contrast image was obtained from an unstained biological sample under a thin carbon film. The image contrast is highest at a low acceleration of 1.5 kV at the 40 nm carbon film (Figs. 1 and 2). These images are similar to transmission images, depending on the sample volume rather than the surface, as with the images of general SEM (Fig. 3). Therefore, images from various angles could be used to construct a 3D model.

Our high contrast images were generated by an indirect mechanism. The sample of bacteria was attached to the lower side of the 40 nm carbon film. The electron beam radiated to the top of the carbon film; the SE signals were mainly generated from a few nanometers under the electron beam spot [18], and the electrons at the low accelerating voltage were largely absorbed by the 40 nm carbon film [16,17]. Previously, many groups have reported the transmission of low energy electrons through thin carbon film [15–17,19]. In these studies, approximately 14% of electrons were transmitted through a carbon film of 40 nm at 1.5 kV [16]. Therefore, a few electrons hit the lower side of the sample through the carbon film by scattering. Under this condition, it is hard to detect a direct signal from the biological sample. We therefore examined the effects at the lower surface of the carbon film. The high contrast of bacteria completely disappeared when the space at the lower side of the sample was closed (Fig. 4C and D). These results strongly suggested that the high contrast image is generated by the SE signal from the lower surface (Fig. 4E). If the electron beam irradiates the thin carbon film, the electrons are scattered in the film, and are randomly diffused. The scatter area of the electrons reached the lower side of the 40 nm carbon film at 1.5 kV. Therefore, both SE signals from top and lower surfaces were detected (Fig. 4E, left). If the electron beam radiates to the lower side of the sample position, the SE signal from the lower surface is sharply reduced by the sample (Fig. 4E, center). Therefore, the sample is shown in clear dark contrast. At this contrast, we propose to name the image as the *i*ndirect *s*econdary *e*lectron *c*ontrast (ISEC) image.

At the upper side of the sample, the electrons are scattered within the sample and are unable to reach the lower surface. Therefore, the SE signal from the lower surface is sharply reduced, this is similar to the lower side sample image (Fig. 4E, right). How-

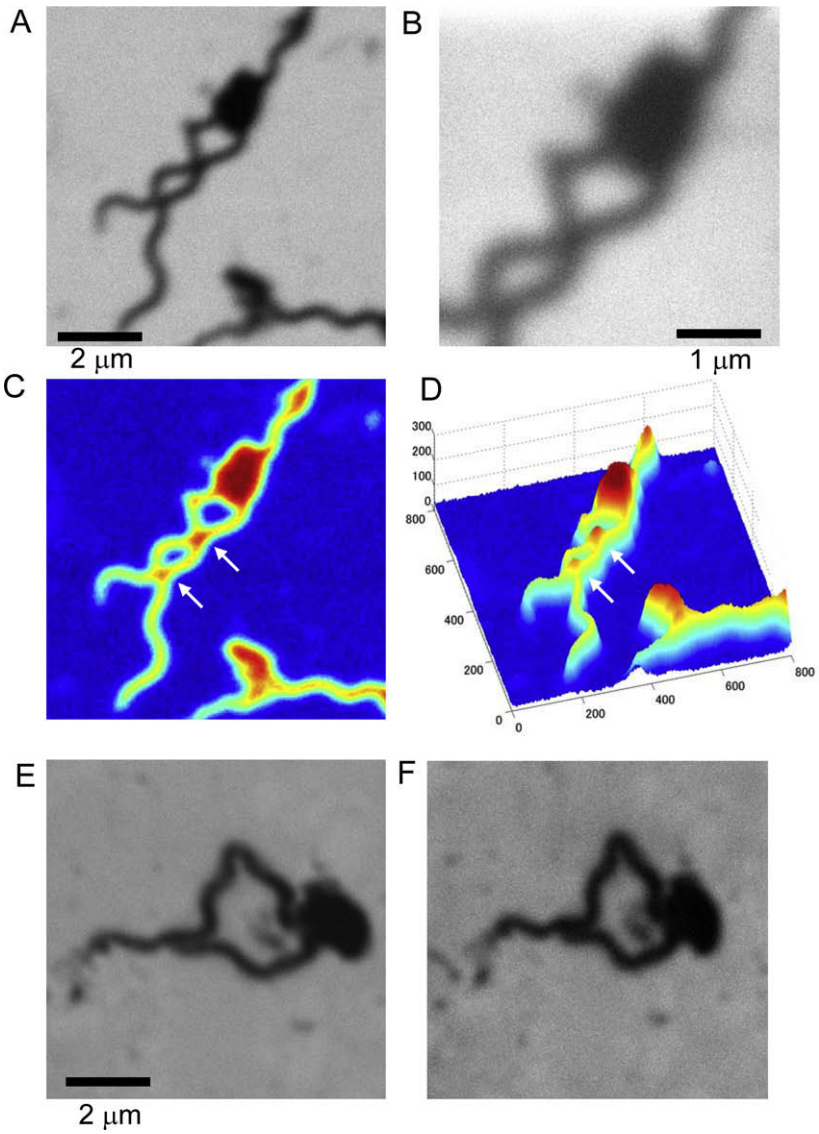

Fig. 3. The features of the high contrast images of bacteria under the carbon film. (A) Image of a typical bacterium at 1.5 kV, at a magnification of 10,000×. The scale bar represents 2 μm. (B) A bacterium from (A) after four additional images have been taken at a magnification of 10,000×, and its body region taken five times at 20,000×. After a total of nine scans, the bacterium does not appear to have been damaged. The scale bar represents 1 μm. (C) Fused color image of a bacteria of (A). Its body is dome-shaped. The white arrows show where the flagella cross, which are almost two times higher than the other flagella positions. (D) A 3D map of the bacteria. The cross point of the flagella, which were identified as being clearly higher than other position. (E) The flat stage image of a bacterium. The scale bar represents 2 μm. (F) Tilted at 30° to the left side. The aspect of the body and flagella has changed.

ever, the electron damage to the upper side of the sample is higher than that to the lower side. With acceleration voltages higher than 10 kV, many electrons pass through the carbon film. At voltages lower than 0.7 kV, all electrons are absorbed by the carbon film. Therefore, there is no dark contrast under either condition. For our working hypothesis, the resolution will be increased using the high-resolution field-emission SEM with a thinner carbon film.

The damage to the lower side of the sample is approximately one tenth lower than the damage to the upper side. Additionally, the low acceleration of 1.5 kV also contributes to preventing damage to the biological sample. However, there are still problems associated with the damage from the vacuum. One of our approaches to this problem is to use trehalose solution in the wash out. Biological samples treated with trehalose are protected from cryopreservation, freeze-drying, and oxidative stress [20–24]. The protective mechanisms of the trehalose comprise three categories, water replacement, glass formation, and chemical stability [24]. Therefore, trehalose solution is well suited for the preparation of biological sample for EM.

In conclusion, the unstained bacterial sample under the 40 nm carbon film gave a high contrast image, detected by the SE signal at a low acceleration voltage of 1.5 kV. The high contrast image is created from the SE signal from the lower surface of carbon film. There is very little damage to the sample, and the image is similar to the transmission image, dependent on the sample volume. Our novel method can be easily utilized to observe various biological samples of bacteria, viruses, and protein complexes.

Acknowledgments

This work was supported by PRESTO of the Japan Science and Technology Agency and by KAKENHI of the grant in aid for scientific research (B).

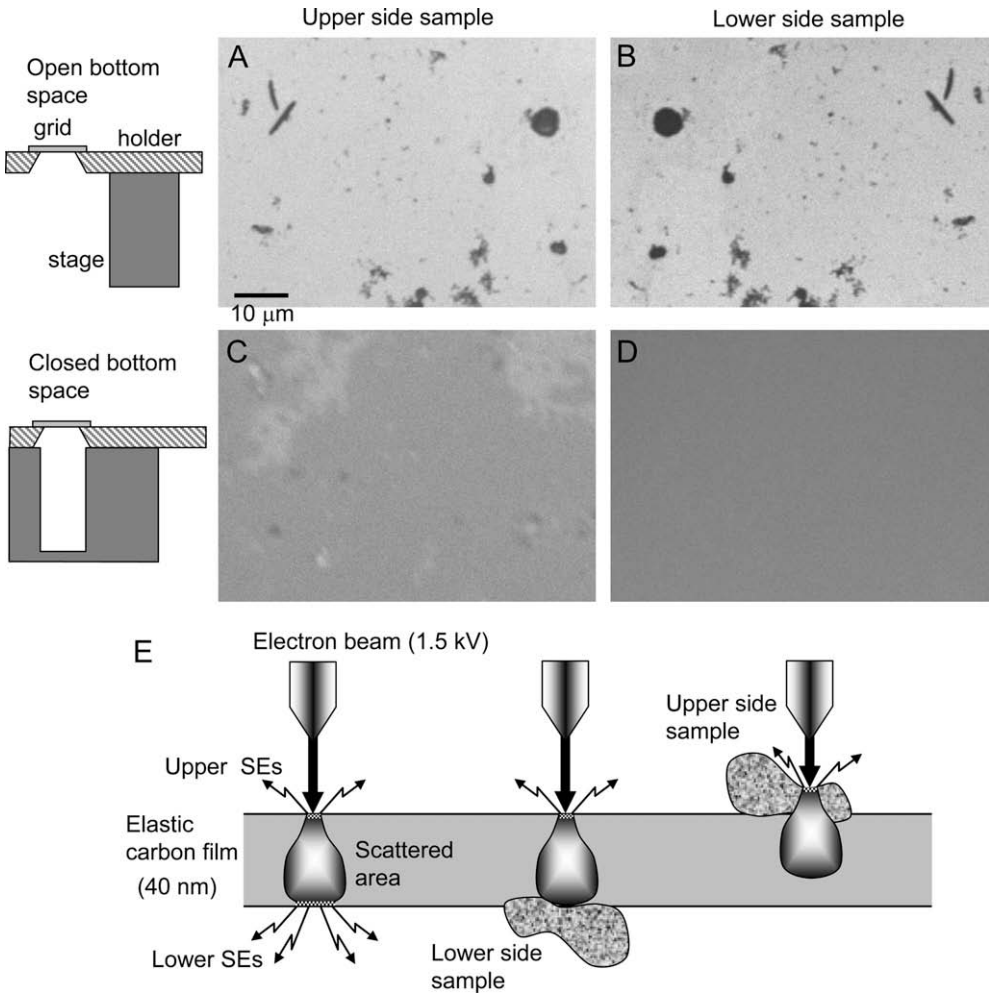

Fig. 4. Comparison of the image contrast with a closed and open bottom space at 1.5 kV. (A) Image of the bacteria with the open space stage. The bacteria on the carbon film exhibited clear black contrast. (B) Image of bacteria under the carbon film located on the open stage exhibiting clear black contrast. (C) Image of the bacteria with the bottom space closed by an aluminum tube. The contrast of the image of the bacteria on the carbon film is very weak. (D) Image of the bacteria under the carbon film on the aluminum tube. The contrast has completely disappeared. (E) Schematic representation of the high contrast mechanism for viewing biological samples under a thin carbon film at 1.5 kV. If the electron beam irradiates the thin carbon film, the electrons are scattered within the carbon film, which randomly diffuses them. The scatter area is close to the lower surface of the carbon film. Therefore, SE signals from the upper and lower sides are detected (left). If the electron beam irradiates the lower side of the sample, the SE signal from the lower surface is sharply decreased by the sample (center). In the upper side sample position, the electrons are scattered within the sample, and do not reach the lower surface. Therefore, the SE signal from the lower side sharply decreases (right).

References

[1] P.M. Motta, S. Makabe, T. Naguro, S. Correr, Oocyte follicle cells association during development of human ovarian follicle. A study by high resolution scanning and transmission electron microscopy, Arch. Histol. Cytol. 57 (1994) 369–394.

[2] J.G. Duckett, R. Ligrone, The formation of catenate foliar gemmae and the origin of oil bodies in the liverwort *Odontoschisma denudatum* (Mart.) dum (Jungermanniales): a light and electron microscope study, Ann. Bot. 76 (1995) 405–419.

[3] N. Minoura, S.I. Aiba, M. Higuchi, Y. Gotoh, M. Tsukada, Y. Imai, Attachment and growth of fibroblast cells on silk fibroin, Biochem. Biophys. Res. Commun. 208 (1995) 511–516.

[4] S.R. Richards, R.J. Turner, A comparative study of techniques for the examination of biofilms by scanning electron microscopy, Water Res. 18 (1984) 767–773.

[5] R. Lamed, J. Naimark, E. Morgenstern, E.A. Bayer, Scanning electron microscopic delineation of bacterial surface topology using cationized ferritin, J. Microbiol. Methods 7 (1987) 233–240.

[6] A.N. Hassan, J.F. Frank, M. Elsoda, Observation of bacterial exopolysaccharide in dairy products using cryo-scanning electron microscopy, Int. Dairy J. 13 (2003) 755–762.

[7] P. Allan-Wojtas, L.T. Hansen, A.T. Paulson, Microstructural studies of probiotic bacteria-loaded alginate microcapsules using standard electron microscopy techniques and anhydrous fixation, LWT-Food Sci. Technol. 41 (2008) 101–108.

[8] L. Vitkov, W.D. Krautgartner, M. Hannig, Bacterial internalization in periodontitis, Oral Microbiol. Immunol. 20 (2005) 317–321.

[9] Y.W. Han, W. Shi, G.T.J. Huang, S.K. Haake, N.H. Park, H. Kuramitsu, R.J. Genco, Interactions between periodontal bacteria and human oral epithelial cells: *Fusobacterium nucleatum* adheres to and invades epithelial cells, Infect. Immun. 68 (2000) 3140–3146.

[10] P.E. Kolenbrander, R.N. Andersen, D.S. Blehert, P.G. Egland, J.S. Foster, R.J. Palmer Jr., Communication among oral bacteria, Microbiol. Mol. Biol. Rev. 66 (2002) 486–505.

[11] P.E. Kolenbrander, R.N. Andersen, L.V.H. Moore, Coaggregation of *Fusobacterium nucleatum*, *Selenomonas flueggei*, *Selenomonas infelix*, *Selenomonas noxia*, and *Selenomonas sputigena* with strains from 11 genera of oral bacteria, Infect. Immun. 57 (1989) 3194–3203.

[12] M. Yamada, A. Ikegami, H.K. Kuramitsu, Synergistic biofilm formation by *Treponema denticola* and *Porphyromonas gingivalis*, FEMS Microbiol. Lett. 250 (2005) 271–277.

[13] M.J. Caimano, K.W. Bourell, T.D. Bannister, D.L. Cox, J.D. Radolf, The *Treponema denticola* major sheath protein is predominantly periplasmic and has only limited surface exposure, Infect. Immun. 67 (1999) 4072–4083.

[14] J.C. Fenno, M. Tamura, P.M. Hannam, G.W.K. Wong, R.A. Chan, B.C. McBride, Identification of a *Treponema denticola* OppA homologue that binds host proteins present in the subgingival environment, Infect. Immun. 68 (2000) 1884–1892.

[15] R.G. Steinhardt, J. Hudis, M.L. Perlman, Attenuation of low-energy electrons by solids: results from X-ray photoelectron spectroscopy, Phys. Rev. B 5 (1972) 1016–1020.

[16] C. Martin, E.T. Arakawa, T.A. Callcott, J.C. Ashley, Low energy electron attenuation length studies in thin amorphous carbon films, J. Electron Spectrosc. Relat. Phenom. 35 (1985) 307–317.

[17] J.C. Ashley, Interaction of low-energy electrons with condensed matter: stopping powers and inelastic mean free paths from optical data, J. Electron Spectrosc. Relat. Phenom. 46 (1988) 199–214.
[18] J. Goldstein, D.E. Newbury, D.C. Joy, C.E. Lyman, P. Echlin, E. Lifshin, L.C. Sawyer, J.R. Michael, Scanning Electron Microscopy and X-ray Microanalysis, Plenum Publishers, New York, 2003.
[19] M. Dapor, Monte Carlo simulation of electron depth distribution and backscattering for carbon films deposited on aluminium as a function of incidence angle and primary energy, Nucl. Instrum. Methods Phys. Res. B 228 (2005) 337–340.
[20] J.H. Crowe, L.M. Crowe, J.F. Carpenter, A.S. Rudolph, C.A. Wistrom, B.J. Spargo, T.J. Anchordoguy, Interactions of sugars with membranes, Biochim. Biophys. Acta 947 (1988) 367–384.
[21] J.H. Crowe, F. Tablin, W.F. Wolkers, K. Gousset, N.M. Tsvetkova, J. Ricker, Stabilization of membranes in human platelets freeze-dried with trehalose, Chem. Phys. Lipids 122 (2003) 41–52.
[22] A. Eroglu, M.J. Russo, R. Bieganski, A. Fowler, S. Cheley, H. Bayley, M. Toner, Intracellular trehalose improves the survival of cryopreserved mammalian cells, Nat. Biotechnol. 18 (2000) 163–167.
[23] J.V. Ricker, N.M. Tsvetkova, W.F. Wolkers, C. Leidy, F. Tablin, M. Longo, J.H. Crowe, Trehalose maintains phase separation in an air-dried binary lipid mixture, Biophys. J. 84 (2003) 3045–3051.
[24] R.S. Herdeiro, M.D. Pereira, A.D. Panek, E.C.A. Eleutherio, Trehalose protects *Saccharomyces cerevisiae* from lipid peroxidation during oxidative stress, Biochim. Biophys. Acta 1760 (2006) 340–346.